Quantifying the structural characteristics and hydraulic properties of shallow Entisol in a hilly landscape**

Cuiting Dai[1], Yaojun Liu[2], Tianwei Wang[1], Zhaoxia Li[1]*, Yiwen Zhou[1], and Jun Deng[1]

[1]College of Resources and Environment, Huazhong Agricultural University, No.1 Shizishan Street, Hongshan District, 430070, Wuhan, China
[2]School of Geographic Sciences, Hunan Normal University, Mulanlou, 36 Lushan Rd., Yuelu District, Changsha, 410081, Hunan, China

Abstract. Entisols are widely distributed in the hilly areas of southern China. They are affected by serious soil erosion and extensive agricultural activities, the structural and hydraulic properties of particular Entisols may differ. Characterizing soil structure and hydraulic properties is important with regard to the development of an understanding of the hydrology and ecosystem functions of shallow Entisols. X-ray computed tomography was used to characterize and quantify the soil pore structure under four typical land use types (cropland, grassland, tea orchard and forest land) from a hilly landscape in South China and the hydraulic properties of the soil including its saturated hydraulic conductivity and water retention curve were measured. The results showed that the soils under the grassland retained 14 and 21% more water at saturation than those under the cropland and tea orchard, respectively. The Entisol in the forest land had a significantly larger macroporosity ($0.214 \ mm^3 \ mm^{-3}$) compared with that in the cropland ($0.117 \ mm^3 \ mm^{-3}$) and tea orchard ($0.131 \ mm^3 \ mm^{-3}$). The contribution of pores with a diameter >4 mm as compared to the total computed tomography derived porosity was 62.4% in the forest land, while this size class contributed 69 and 47.3% to the total porosity in the tea orchard and grassland, respectively. The saturated hydraulic conductivity value was well correlated with the degree of anisotropy and the fractal dimension.

Keywords: land use, X-ray computed tomography, structure, soil hydraulic properties, Entisols

INTRODUCTION

Entisols are widely distributed, they account for 16% of the ice-free land area in the world (Bruns, 2014). They are commonly found on steep slopes with little profile development (A-C or A-R profile). In the hilly area of southern China, soils are heavily affected by severe soil erosion and also by the nature of parent material/rock, thus Entisols with a shallow soil layer and also a poor soil structure are widely distributed. The physical state of the soil (*e.g.* soil layering, structure and hydraulic properties) plays an important role in many processes such as infiltration, surface runoff, gaseous exchanges and susceptibility to soil erosion (Rabot *et al.*, 2018). Hence, it is essential to characterize the structure and hydraulic properties of the soil to provide insight into the hydrology and ecosystem functions of Entisols.

Soil hydraulic properties are controlled by many factors such as soil thickness and structure. Woolhiser *et al.* (2006) found that the shallow soil in the upper slope had a higher hydraulic conductivity and drainage velocity thereby causing bedrock infiltration. Lin *et al.* (2008) also observed larger hydraulic conductivities and infiltration capacities in soils with shallow thickness values as compared to thick soils. As a crucial attribute of the soil structure, soil pores are believed to greatly affect soil hydraulic properties (Vogel, 2000; Leuther *et al.*, 2019). Saturated hydraulic conductivity (K_{sat}) is highly influenced by the pore size, continuity and connectivity of the

pore structure network (Larsbo *et al.*, 2014). A continuous pore network facilitates a rapid water flow thus resulting in a greater degree of hydraulic conductivity (Rezanezhad *et al.*, 2009; Alaoui *et al.*, 2011). Soil pores are sensitive to human activities associated with land use/cover or tillage (Luo *et al.*, 2010a; Abdollahi *et al.*, 2014; Borges *et al.*, 2019). Soil pore characteristics including porosity, continuity and size distribution may be significantly different under natural soils as compared to continuously cultivated soils.

Previous studies have reported that land use management may alter the structural properties of the soil such as changes in pore size distributions which regulate water retention and storage capacity (Zhou *et al.*, 2008; Zhang *et al.*, 2016; Wang *et al.*, 2019). Plant roots can establish a continuous pore system in the absence of anthropogenic disturbance. Living plants or crops growing on the soil surface may, in certain circumstances, facilitate water infiltration by reducing the effect of rainfall. Rooting processes varied with different types of plants or crops which are believed to affect the formation of pores (Kravchenko *et al.*, 2011). Zeng *et al.* (2013) found an accelerated change in the number of macropores in an increasingly degraded condition. Van der Kamp *et al.* (2003) reported an improved macropore network in the perennial brome grass soil as compared to cropland, thus increasing the infiltration rate. The effects of land use on soil pore characteristics have been investigated in different soils and areas such as a Loess plateau gully area in northern China (Qiao *et al.*, 2021), a Calcic Kastanozem degraded rangeland in central Iran (Baranian Kabir *et al.*, 2020), a Haplic Luvisol agricultural field in the Czech Republic (Kodesova *et al.*, 2011), and a paddy and upland field in a Red soil area in China (Zhang *et al.*, 2018). However, relevant information concerning the shallow Entisols of the hilly area is limited.

Traditionally, soil pore characteristics are obtained indirectly from soil water information such as soil water retention curves or measured using mercury intrusion porosimetry or observed directly using the scanning electron microscopy method combined with digital image analysis (Vogel, 2000; Pagliai *et al.*, 2004; Zhu *et al.*, 2020). However, these methods are time consuming and destructive, also none of them can provide the subtle features of the soil pore networks (Schlüter *et al.*, 2019). In recent decades, X-ray computed tomography (CT) has been successfully used to characterize and quantify the soil 3D pore structure (Luo *et al.*, 2010b; Katuwal *et al.*, 2015; Rabot *et al.*, 2018). This technique provides a very powerful method which may be used to analyse pore characteristics at a favourable resolution without destroying the original structure of the soil (Schlüter *et al.*, 2018; Diel *et al.*, 2019; Feng *et al.*, 2020). Macropores and their geometrical characteristics may be revealed by using X-ray CT and imaging analysis (Luo *et al.*, 2010a). The direct reconstruction, visualization and quantification of 3D macropore networks derived from X-ray CT allow for the correlation of macropore characteristics to water movement and solute transport in soils (Katuwal *et al.*, 2015; Galdos *et

al., 2019; Zhang *et al.*, 2019). Therefore, the quantification of macropore characteristics in soils can be used to improve our understanding of flow and pollutant transport processes.

The objectives of our study were (1) to quantify and characterize the pore structures of shallow Entisol under different land uses in the hilly landscape of southern China using the X-ray CT method, (2) to investigate the effects of land use on saturated hydraulic conductivity (K_{sat}) and water retention, and (3) to analyse the quantitative relationships between soil hydraulic conductivity and CT-derived pore characteristics.

MATERIALS AND METHODS

The study site was located in a hilly part of southern China near the Three Gorges Dam (30°38′~31°11′N, 110°18′~111°0′E) (Fig. 1). The climate is classified as subtropical monsoon with a yearly mean rainfall of 1164 mm, distributed mainly between April and September. The average annual temperature in this area is 16.8°C, and the annual frost-free period is approximately 306 days. With its long-term geological evolution and external erosivity of water and wind, this area has many mountainous geomorphological landscapes. The soil is formed by shales with intense physical weathering. The dominant soil textural class is loam and shallow Entisols are widely distributed in the study area. The land use in the area is mainly represented by cropland, forest, tea orchard, and wild grassland.
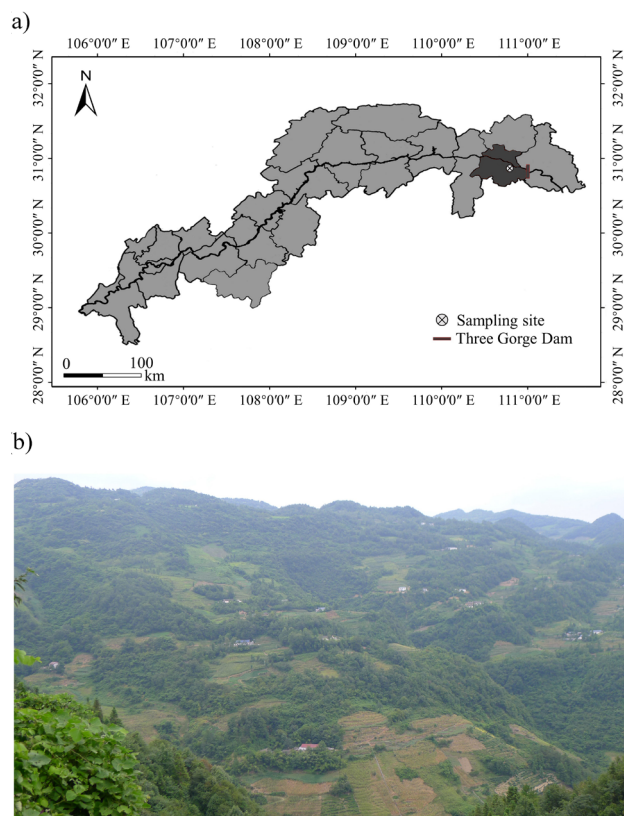
Fig. 1. Location of the study area, with (a) location map of the study area in South China, (b) representative landscape of the study site.
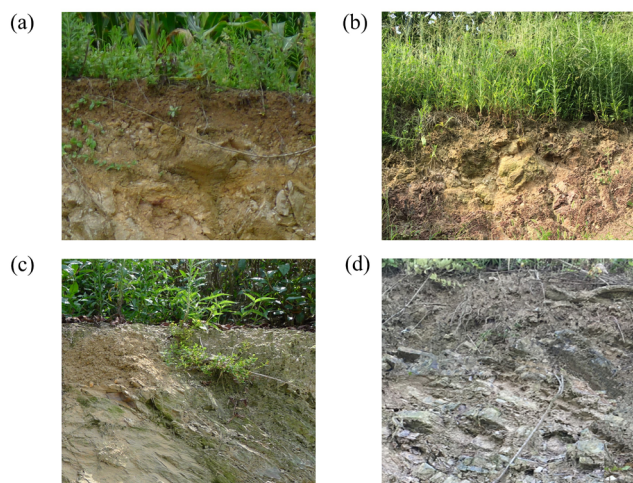
Fig. 2. Representative profiles of the studied land-use types; (a) Cropland, (b) Grassland, (c) Tea orchard and (d) Forest land.

Three sites were selected and the topography, soil and environmental conditions of each site were relatively similar. Each site contained four land use types: cropland, grassland, tea orchard and forest land (Fig. 2). Six sampling points were selected randomly from which to collect soil samples for each land use type. No rain fell at least one week before the samples were taken. Given the shallow condition of the soil layer, undisturbed soil columns were collected using 10 cm length and 10.8 cm internal diameter polyvinyl chloride (PVC) cylinders. In order to avoid disturbance, the soil was first trimmed to the cylinder size and then covered with the PVC tube. The soil columns were carefully sealed with plastic film and wrapped with sponge at the top and bottom to avoid any disturbance during transport and then stored at 4°C before CT scanning took place. In addition, intact soil cores (18 replicates for each land use type) with a diameter of 5 cm and a height of 5 cm were sampled from the topsoil of each sampling point. The bulk soil of each land use type was also collected and air dried before further analysis.

The basic soil physical and chemical properties under different land uses were measured in the laboratory using standard procedures. The soil texture was determined via the wet sieving-pipette method (Gee and Or, 2002). The total soil organic carbon (SOC) was measured using the potassium-dichromate ($K_2Cr_2O_7$) oxidation method (Walkley and Black, 1934). Soil water retention was determined in intact cores using the centrifuge method. The cores were saturated for 24 h by immersing them stepwise in water and then they were drained sequentially at nine water potential steps (0, –0.4, –2.5, –5, –10, –20, –33, –100 and –1500 kPa). The Van Genuchten model was fitted to the measured soil water retention curve using RETC software (van Genuchten, 1980). The saturated hydraulic conductivity (K_{sat}) was measured using the constant head method described by Ilek and Kucza (2014). The bulk density was measured using the

core method (Blake and Hartge, 1986) by oven-drying the cores for at least 24 h at 105°C. Finally, the rock fragment content (RFC) was determined using the drainage method.

All of the undisturbed soil columns were placed horizontally on the bench and spiral scanned using an industrial X-ray CT scanner (nanoVoxel 4000, Sanying Precision Instruments Co., Ltd, China). In order to minimize the ring artifacts caused by beam hardening, a 1 mm CaF_2 filter was placed between the soil samples and the X-ray source. The scanning voltage and X-ray tube current was set to 190 kV and 140 μA to optimize spatial resolution and image contrast. After reconstruction, the 16-bit grayscale three-dimensional data were obtained at a resolution of 0.06 mm. Therefore, only macropores larger than 0.06 mm were quantified in this study. During sampling and transportation, the tops and bottoms of the soil samples were unavoidably disturbed. Therefore, a central part of the columns was selected as the region of interest (ROI) with 1200×1200×1200 voxels for further pore structure analysis and pore network modelling, corresponding to a volume of 72×72×72 mm.

Image processing and analysis were performed using Avizo 9.7 (Hillsboro, OR, USA) software and for the most part followed the procedures used by (Luo *et al.*, 2010a). A non-local means filter was used to minimize the image noise, and an unsharp mask was applied for edge enhancement (Buades *et al.*, 2005; Schlüter *et al.*, 2014). Thresholding is based on the grey scale and edge information of the entire soil sample and was applied to segment the macropores and the soil matrix (Lamandé *et al.*, 2013). After segmentation, the morphological 'Closing' module of Avizo was performed on the binary images to fill the small holes inside the pores and smooth the pore boundaries. Due to the limitations of image resolution (0.06 mm), the pores for further analysis only include pores larger than 0.06 mm in diameter, which are considered to be macropores in this study. The shape of the soil macropore system was characterized by the degree of anisotropy (Ketcham, 2005).

After segmentation, the macropore structures were reconstructed and visualized using Avizo 9.7. The connected macropores were extracted using the 'Axis Connectivity' module of Avizo 9.7. The porosity of the sample, including macroporosity and connected macroporosity was calculated using the 'Volume Fraction' module. Macropore characteristics including pore-size distribution (classified by equivalent diameter), length density, specific surface area, connectivity (Euler number), and the degree of anisotropy were calculated using the 'Label Analysis' module of Avizo 9.7. The 'Sieve analysis' module in Avizo was measured and the equivalent diameter was used to place macropores into different size classes (<0.5, 0.5-1, 1-2, 2-3, 3-4, and >4 mm). The fractal dimension of the pore structure was measured using the 'Fractal Dimension' module of Avizo. When the pore network structure becomes more complex, the fractal dimension increases. Therefore, the fractal dimension is used to quantify the complexity or tortuosity of the pore structure (Dal Ferro *et al.*, 2013).

A statistical analysis was performed using IBM SPSS statistical software (Version 21.0, SPSS Inc., Chicago, IL, USA). Differences in the macropore structures of the soil columns among the different land use types were interpreted through a one-way analysis of variance (ANOVA) and least significant difference (LSD) test using a 95% confidence level. The relationships between soil hydraulic conductivity and pore characteristics were evaluated using linear regression analysis and Pearson correlation.

RESULTS

The means and standard deviations of the soil physicochemical properties under different land uses are summarized in Table 1. According to USDA classification, the studied Entisols were classified as loam or clay loam. The soil bulk density varied significantly between the different land use types (p<0.05). The results show that the bulk density for the four land use types varied as follows: tea orchard > cropland > grassland > forest land. The highest total porosity values were observed in the forest land, but the total porosities of the forest and grassland were statistically similar. The rock fragment content under the tea orchard and forest land was significantly larger than that of the cropland and grassland (p<0.05). Significantly less soil organic carbon was observed in the tea orchard (p<0.05). Although the means of the soil organic carbon were higher in the forest land as compared to those of the cropland and grassland, the difference was not significant.

The fitting of van Genuchten parameters using the RETC program is shown in Table 2. The water retention curves are illustrated in Fig. 3. A larger saturated water content and higher retention ability was found at the grassland site as compared to the cropland and tea orchard areas. The soil under the grassland retained 14 and 21% more water under saturation conditions than those under the cropland and tea

orchard, respectively. The differences in the saturated water content and retention characteristics between soils under the grassland and the forest land were not significant at all of the measured water pressures. The differences in water retention among the four land uses were only significant (p<0.05) at higher soil water pressures (0, –0.4, –2.5, and –5.0 kPa), which indicates that the effects of land use on water retention are more sensitive to larger pores. The soil at the grassland had a significantly higher water retention capacity compared to that in the cropland and the tea orchard (Fig. 3). Saturated hydraulic conductivity (K_{sat}) differed significantly between the various land uses (p<0.05; Table 1). The forest land enhanced the K_{sat} (23.5 mm h^{-1}) value more than that of the cropland (11.5 mm h^{-1}) and the tea orchard (8.4 mm h^{-1}).

The soil macropore characteristics of the four land use types are listed in Table 3. The Entisol used as forest land (0.214 mm^3 mm^{-3}) had a significantly larger macroporosity as compared with that in the cropland (0.117 mm^3 mm^{-3}) and tea orchard (0.131 mm^3 mm^{-3}), (p<0.05, Table 3). The CT-derived macroporosity was higher in the grassland as compared with the cropland and tea orchard areas, but the differences were not statistically significant. A similar trend was found in connection with macroporosity, the highest value of this parameter was determined under the forest land among the four land uses. The cropland soil had the highest pore length density (0.159 mm^2) and the lowest specific surface area (0.601 mm^2 mm^{-3}). No significant differences were found in length density and the specific surface between the cropland soil and the grassland and tea orchard soils (p>0.05). The forest land had a significantly lower degree of anisotropy as compared to the tea orchard. The fractal dimension was measured to account for the heterogeneity of the spatial distribution of the macropore structures. The results showed that cropland, grassland and forest land had

Table 1. Measured soil properties (mean ± standard deviation) under different land uses

Land use	Sand (%)	Silt (%)	Clay (%)	USDA soil texture	Bulk density (g cm^{-3})	Total porosity (%)	RFC (%)	SOC (g kg^{-1})	K_{sat} (cm h^{-1})
Cropland	44.3±3.1a	32.0±6.1a	23.7±3.5b	Loam	1.46±0.01ab	44.7±0.5ab	22.3±1.3a	20.0±2.4a	11.5±3.9b
Grassland	43.2±2.0a	29.2±2.1a	27.6±0.2a	Clay loam	1.34±0.17ab	49.3±6.4ab	23.4±4.9a	21.6±2.9a	22.7±7.7a
Tea orchard	46.5±2.4a	30.9±2.7a	22.6±0.8b	Loam	1.54±0.06a	42.1±2.2b	31.4±6.3a	14.9±1.3b	8.4±1.3b
Forest land	45.5±1.0a	29.4±1.3a	25.1±1.5ab	Loam	1.25±0.20b	52.7±7.5a	27.7±5.1a	23.3±2.3a	23.5±0.3a
F-value	1.20	0.43	3.79	–	2.65	2.62	2.08	7.40	9.33
p-value	0.371	0.734	0.059	–	0.121	0.123	0.182	0.011	0.005

RFC – rock fragment content; SOC – soil organic carbon; K_{sat} – saturated hydraulic conductivity. In each row, figures with different letters are significantly different at p<0.05.

Table 2. Van Genuchten soil hydraulic parameters obtained using the RETC program

Land use	θr^B (cm^3 cm^{-3})	θs^A (cm^3 cm^{-3})	α^B (cm^{-1})	n^B
Cropland	0.066±0.006abc	0.334±0.021b	0.013±0.002a	1.446±0.042a
Grassland	0.077±0.006a	0.412±0.019a	0.014±0.001a	1.422±0.036a
Tea orchard	0.061±0.003c	0.324±0.026b	0.015±0.000a	1.406±0.021a
Forest land	0.074±0.005ab	0.359±0.011b	0.013±0.002a	1.458±0.035a
F-value	6.45	11.50	1.40	1.374
p-value	0.16	0.003	0.312	0.319

A – represents measured values; B – represents optimized values. Other explanations as in Table 1.
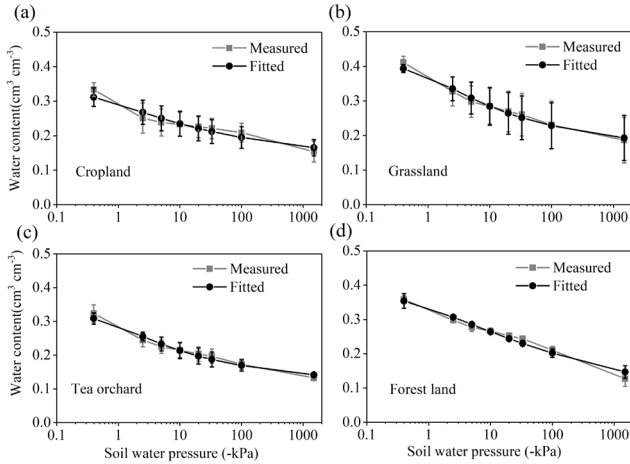
Fig. 3. Measured soil water retention curves under different land uses.

Fig. 4. Typical CT scanning images for the soil under different land uses; (a) orthogonal cross-sections in which black represents the macropores and yellow represents the soil matrix, (b) vertical cross-sections.

significantly larger fractal dimensions as compared to tea orchard (p<0.05). The highest fractal dimension was recorded in the forest land with a mean value of 2.421, indicating that it had the most complex pore structure. The connectivity of the pore structures is described by the Euler number. A high degree of variability in connectivity was observed for each type of land use. The forest land had the lowest Euler number and the best connectivity. The differences in the Euler number among the four land uses was only significant between cropland and forest land (p<0.05).

In order to characterize the pore-size distribution for different land uses, soil porosity as a function of pore size (<0.5, 0.5-1, 1-2, 2-3, 3-4, >4 mm) and pore volume (<0.001, 0.001-0.01, 0.01-0.1, 0.01-1, 1-10, 10-100 and >100 mm^3) is depicted in Fig. 5. The distribution of CT-measured pores according to the diameter or volume was relatively similar among the four land use types. The CT-derived porosity with a diameter of less than 3 mm was the highest in the cropland, but the difference was only significant for pore diameters of 2-3 mm (p<0.05). The forest land had significantly larger porosities for the pore-size class of >3 mm. For the pore-size class of >4 mm, a trend of forest land > tea orchard > grassland > cropland in porosities was observed. The contribution of pore diameter >4 mm to the total CT-derived porosity was 62.4% in the forest land, while this size class contributed 69 and 47.3% to the total porosity in the tea orchard and grassland, respectively. A pore diameter

of <1 mm contributed to the smallest portion of the total porosity derived from CT (3.9, 3.6, 4.0 and 1.3% in cropland, grassland, tea orchard and forest land, respectively). The differences in the CT-derived porosities differentiated according to pore diameter among the four land uses and were only significant for pores larger than 2 mm. The primary contribution to the total porosity as measured by CT (72.4, 74.4, 45.5 and 72.8% in cropland, grassland, tea orchard and forest land, respectively) was made by pores with a volume of 10-100 mm^3 in all the land uses.

In order to explore the influencing factors of K_{sat}, the relationships between the K_{sat} values and soil pore characteristics were analyzed (Fig. 6). The obtained R^2 (coefficient of determination) ranged between 0.15 and 0.66. The K_{sat} value increased to a significant extent with the increase in macroporosity and connected macroporosity (p<0.05) derived using CT, the specific surface area (p<0.05) and the fractal dimension (p<0.01), whereas it decreased significantly with the increasing degree of anistropy (p<0.01). Both length density and connectivity showed no significant correlations with K_{sat}.

DISCUSSION

Understanding the characteristics of soil pore systems under different land uses is important for long-term soil sustainability, especially in hilly landscapes susceptible to soil erosion. Our results have shown that the soils of forest

Table 3. X-ray CT derived macropore characteristics under different land uses

Land use	MP (mm^3 mm^{-3})	CMP (mm^3 mm^{-3})	LD (mm^2)	SSA (mm^2 mm^{-3})	DA	Fractal dimension	Euler number
Cropland	0.117±0.021b	0.109±0.023b	0.159±0.022a	0.601±0.062b	0.743±0.060ab	2.385±0.006a	26943±14958a
Grassland	0.152±0.014b	0.146±0.016b	0.138±0.014ab	0.763±0.096ab	0.682±0.090ab	2.413±0.031a	15075±11842ab
Tea orchard	0.131±0.023b	0.124±0.025b	0.148±0.008ab	0.673±0.031ab	0.801±0.021a	2.340±0.002b	13339±12522ab
Forest land	0.214±0.026a	0.210±0.027a	0.129±0.007b	0.752±0.088ab	0.653±0.094b	2.421±0.034a	−2012±2410b
F-value	11.61	10.97	2.54	3.16	2.49	7.56	3.22
p-value	0.003	0.003	0.129	0.086	0.134	0.010	0.083

MP - macroporosity; CMP – connected macroporosity; LD – length density; SSA – specific surface area; DA – degree of anisotropy. Other explanations as in Table 1.
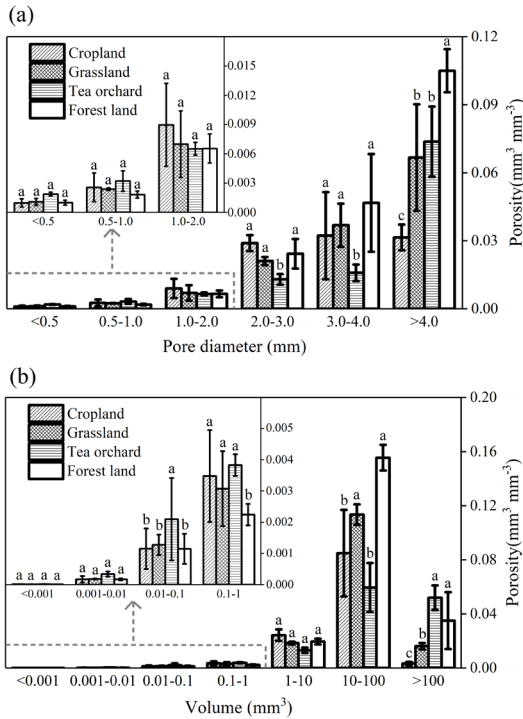
Fig. 5. Distribution of the CT-derived soil porosity as a function of (a) pore diameter, and (b) pore volume for different land uses. Columns with different letters are significantly different at p<0.05.
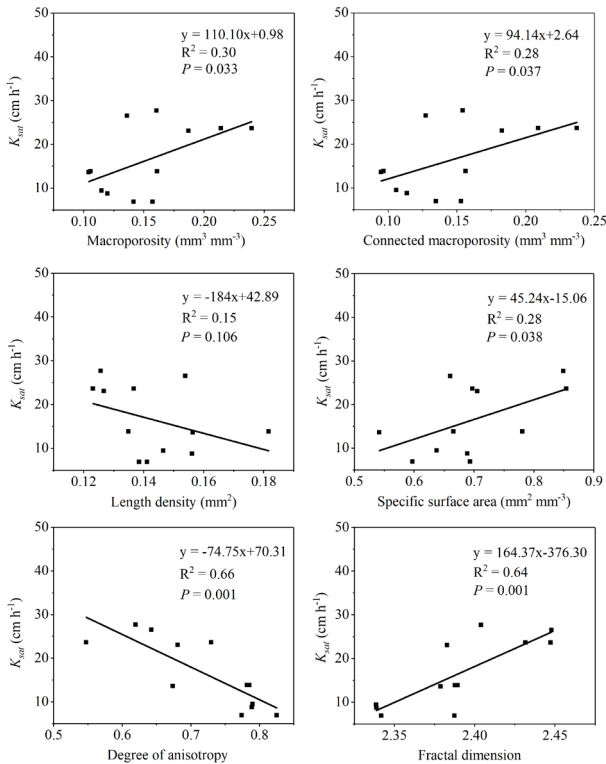
Fig. 6. Relationships between K_{sat} and soil pore characteristics.

land had a significantly greater degree of macroporosity and connected macroporosity than those under crop, grass, and tea land use, this may be attributed to more developed

roots and a greater accumulation of organic matter in forested land. Similarly, Udawatta *et al.* (2008) reported that the soils under natural grassland had a much higher porosity value and larger macropores than the soils used in cropland. The roots in the grassland, tea orchard and forest land can develop large pores, cracks, and voids thereby increasing porosities (Hu *et al.*, 2016; Zhao *et al.*, 2017). Land use also influence the pore-size distribution. In this study, the large macropores (>3 mm) made the largest contribution to the total porosity as measured by CT. The changes in pore-size distribution and volume can have a substantial impact on soil air and water movement, which are important for many soil processes and functions (Chandrasekhar *et al.*, 2019; de Oliveira *et al.*, 2021). The porosity of very large macropores (>100 mm³) was considerably higher at the tea orchard site than at the cropland site (Fig. 5b). Our results also found that land use effects on pore size were more significant on large macropores with diameters of >4 mm (Fig. 5a), indicating that large macropores (>4 mm) responded more rapidly and to a greater degree to human disturbances as compared to smaller pores.

Different land uses can also have different effects on pore morphology. The degree of anisotropy was much larger in the soils under the tea orchard (0.801) than the forest land (0.653). The fractal dimension provides useful detail about the pore space filling properties and is characterized as an index of the complexity or tortuosity of a geometric shape. The fractal dimension for a 3D porous system ranges from 2 to 3, and is directly proportional to the pore complexity (Dal Ferro *et al.*, 2013). In this study, the forest land had higher fractal dimension values which indicated that the pores in the forest land occupied more space and that the pore structure was more complex compared to that of the tea orchard. However, the tea orchard had a significantly (p<0.05) lower fractal dimension as compared to the cropland and grassland areas, thereby indicating that the pore network was more homogeneous. The fractal dimension was higher (2.421 vs 2.385) and the Euler number was lower (–2012 vs 26943) in the forest land compared with that in the cropland, implying that the pore structure was more continuous and intricate in the forest land, which would hinder erosion, promote infiltration, and preserve the soil structure (Udawatta and Anderson, 2008; Luo *et al.*, 2010a; Bienes *et al.*, 2016). The differences in Euler number for all of the treatments were larger than those in the fractal dimension in the same soil samples, showing that the Euler number was more sensitive to variations in the pore networks. Similarly, the findings by Dal Ferro *et al.* (2013) showed that the Euler number was a more sensitive index than the fractal dimension for assessing land management effects. However, the opposite results were reported by Katuwal *et al.* (2015). They proposed that the Euler number was not a fine indicator for quantifying the connectivity of soil pore systems among samples. These contrasting conclusions may be attributed to the contrasting resolutions of the X-ray CT images and also to the

segmentation approaches applied to macropores. Therefore, a good and widely acknowledged approach of segmentation would be a high priority in order to minimize the limitations of imaging analysis for pore morphology (Tabor, 2011; Garbout *et al.*, 2013; Zhao *et al.*, 2017).

Soil hydraulic properties such as the saturated hydraulic conductivity (K_{sat}) and the water retention curve are key elements for controlling water transport and retention in soils. Many studies have described the significant effects of land use on the K_{sat} value (Chen *et al.*, 2009; Price *et al.*, 2010; Shabtai *et al.*, 2014; Kalhoro *et al.*, 2018; Liu *et al.*, 2018). The differences in K_{sat} induced by land use may be rational because the changes in soil properties have been confirmed by many previous studies concerning parameters such as bulk density, soil organic carbon, as well as by soil porous systems as affected by land use (Haruna *et al.*, 2018; Lauber *et al.*, 2008; Murty *et al.*, 2002; Zhang *et al.*, 2019). For the shallow loamy Entisol in our study, significant differences in K_{sat} were observed among different land uses. Some of the soil pore characteristics that were measured such as porosity, the specific surface area, the degree of anisotropy and the fractal dimension were found to affect K_{sat} (Fig. 6). However, the results by Zhang *et al.* (2019) showed that the best relationships between K_{sat} and macropore characteristics were observed with reference to the mean macropore diameter. This may be due to the different soil types (Entisol *vs* Utisol) and management policies examined in these two studies. Significantly greater saturated water contents were observed in the grassland as compared to the other treatments in our study. The effects of land use on water retention were only significant at higher soil water pressures (0, 0.4, –2.5, and –5.0 kPa), which indicated that larger pores are more sensitive to land use. Moreover, the results indicated that land use effects on hydraulic properties are mainly the result of changes in the soil pore structure.

When Entisols are affected by severe erosion and extensive agricultural land use this can lead to structural degradation. Understanding the effects of land use on the structural and hydraulic properties of soil is important for effective land management, sustainable land use and soil productivity improvement. Our study indicates that forest and grassland have a critical importance for conserving soil structural and hydraulic functions. The improvement of soil pore structure can alter the natural hydrological balance of the ecosystem and eventually mitigate water erosion and nutrient loss occurring through runoff from agricultural land use. Improving the pore-size and volume distribution in the topsoils can increase the rate of water infiltration within the soils which in turn reduces surface runoff and water evaporation and increases the water use efficiency of the plant. Exploring best management practices for ameliorating soil pore space in the topsoil is of great importance in the agriculture of hilly areas.

CONCLUSIONS

1. For the most part land use affected large macropores in shallow Entisols. Macropores with diameters larger than 4 mm contributed the most to the total CT-derived porosity under all four land use types.

2. The pore morphology and the quantitative macropore parameters indicated that the Entisols used for forest and grassland had a better soil pore network as compared with that used for cropland.

3. The saturated hydraulic conductivity was well correlated with the total porosity, degree of anisotropy and fractal dimension. We strongly support the concept that soil pores are a significant driver of the variations in soil hydraulic parameters which are induced by land use in hilly areas.

Conflicts of interest: The authors declare no conflict of interest.

REFERENCES

Abdollahi L., Munkholm L.J., and Garbout A., 2014. Tillage system and cover crop effects on soil quality: II. pore characteristics. Soil Sci. Soc. Am. J., 78, 271-279, https://doi.org/10.2136/sssaj2013.07.0302

Alaoui A., Lipiec J., and Gerke H.H., 2011. A review of the changes in the soil pore system due to soil deformation: A hydrodynamic perspective. Soil Tillage Res., 115-115, 1-15, https://doi.org/10.1016/j.still.2011.06.002

Baranian Kabir E., Bashari H., Bassiri M., and Mosaddeghi M.R., 2020. Effects of land-use/cover change on soil hydraulic properties and pore characteristics in a semi-arid region of central Iran. Soil Tillage Res. 197, 104478, https://doi.org/10.1016/j.still.2019.104478.

Bienes R., Marques M.J., Sastre B., García-Díaz A., and Ruiz-Colmenero M., 2016. Eleven years after shrub revegetation in semiarid eroded soils. Influence in soil properties. Geoderma, 273, 106-114, https://doi.org/10.1016/j.geoderma.2016.03.023

Blake G.R. and Hartge K.H., 1986. Bulk density. In: Methods of Soil Analysis, Part 1. Physical and Mineralogical Methods. Agron. Monogr. 9 (Ed. C.A. Black), ASA, https://doi.org/10.2134/agronmonogr9.1.c30

Borges J.A.R., Pires L.F., Cássaro F.A.M., Auler A.C., Rosa J.A., Heck R.J., and Roque W.L., 2019. X-ray computed tomography for assessing the effect of tillage systems on topsoil morphological attributes. Soil Tillage Res., 189, 25-35, https://doi.org/10.1016/j.still.2018.12.019

Bruns M.A., 2014. Sustainable soil health. In: Plant Biotechnology (Eds A. Ricroch, S. Chopra, S. Fleischer). Springer, Cham., https://doi.org/10.1007/978-3-319-06892-3_17

Buades A., Coll B., and Morel J.M., 2005. A non-local algorithm for image denoising. In Proceedings – 2005 IEEE Computer Society Conference on Computer Vision and Pattern Recognition, CVPR 2005.

Chandrasekhar P., Kreiselmeier J., Schwen A., Weninger T., Julich S., Feger K.H., and Schwärzel K., 2019. Modeling the evolution of soil structural pore space in agricultural soils following tillage. Geoderma, 353, 401-414, https://doi.org/10.1016/j.geoderma.2019.07.017

Chen X., Zhang Z., Chen X., and Shi P., 2009. The impact of land use and land cover changes on soil moisture and hydraulic conductivity along the karst hillslopes of southwest China. Environ. Earth Sci., 59, 811-820, https://doi.org/10.1007/s12665-009-0077-6

Dal Ferro N., Charrier P., and Morari F., 2013. Dual-scale micro-CT assessment of soil structure in a long-term fertilization experiment. Geoderma, 204-205, 84-93, https://doi.org/10.1016/j.geoderma.2013.04.012

Diel J., Vogel H.J., and Schlüter S., 2019. Impact of wetting and drying cycles on soil structure dynamics. Geoderma, 345, 63-71, https://doi.org/10.1016/j.geoderma.2019.03.018

Feng Y., Wang J., Bai Z., Reading L., and Jing Z., 2020. Three-dimensional quantification of macropore networks of different compacted soils from opencast coal mine area using X-ray computed tomography. Soil Tillage Res., 198, 104567, https://doi.org/10.1016/j.still.2019.104567

Galdos M.V., Pires L.F., Cooper H.V., Calonego J.C., Rosolem C.A., and Mooney S.J., 2019. Assessing the long-term effects of zero-tillage on the macroporosity of Brazilian soils using X-ray Computed Tomography. Geoderma, 337, 1126-1135, https://doi.org/10.1016/j.geoderma.2018.11.031

Garbout A., Munkholm L.J., and Hansen S.B., 2013. Temporal dynamics for soil aggregates determined using X-ray CT scanning. Geoderma, 204-205, 15-22, https://doi.org/10.1016/j.geoderma.2013.04.004

Gee G.W. and Or D., 2018. Particle-Size Analysis. In: Methods of Soil Analysis: Part 4 Physical Methods, 5.4. (Eds J.H. Dane, G. Clarke Topp). Soil Sci. Soc. Am., Madison, 255-293, https://doi.org/10.2136/sssabookser5.4.c12

van Genuchten M.T., 1980. Closed-Form Equation for Predicting the Hydraulic Conductivity of Unsaturated Soils. Soil Sci. Soc. Am. J., 44, 892-898, https://doi.org/10.2136/sssaj1980.03615995004400050002x

Haruna S.I., Anderson S.H., Nkongolo N.V., and Zaibon S., 2018. Soil Hydraulic Properties: Influence of Tillage and Cover Crops. Pedosphere, 28, 430-442, https://doi.org/10.1016/S1002-0160(17)60387-4

Hu X., Li Z.C., Li X.Y., and Liu L.Y., 2016. Quantification of soil macropores under alpine vegetation using computed tomography in the Qinghai Lake Watershed, NE Qinghai-Tibet Plateau. Geoderma, 264, 244-251, https://doi.org/10.1016/j.geoderma.2015.11.001.

Ilek A. and Kucza J., 2014. A laboratory method to determine the hydraulic conductivity of mountain forest soils using undisturbed soil samples. J. Hydrol., 519(B), 1649-1659, https://doi.org/10.1016/j.jhydrol.2014.09.045

Kalhoro S.A., Xu X., Ding K., Chen W., Shar A.G., and Rashid M., 2018. The effects of different land uses on soil hydraulic properties in the Loess Plateau, Northern China. L. Degrad. Dev., 29, 3907-3916, https://doi.org/10.1002/ldr.3138

van der Kamp G., Hayashi M., and Gallén D., 2003. Comparing the hydrology of grassed and cultivated catchments in the semi-arid Canadian prairies. Hydrol. Process., 17, 559-575, https://doi.org/10.1002/hyp.1157

Katuwal S., Norgaard T., Moldrup P., Lamandé M., Wildenschild D., and de Jonge L.W., 2015. Linking air and water transport in intact soils to macropore characteristics inferred from X-ray computed tomography. Geoderma, 237-238, 9-20, https://doi.org/10.1016/j.geoderma.2014.08.006

Ketcham R.A., 2005. Three-dimensional grain fabric measurements using high-resolution X-ray computed tomography. J. Struct. Geol., 27(7), 1217-1228, https://doi.org/10.1016/j.jsg.2005.02.006

Kodesova R., Jirku V., Kodes V., Muhlhanselova M., Nikodem A., and Žigová A., 2011. Soil structure and soil hydraulic properties of Haplic Luvisol used as arable land and grassland. Soil Tillage Res., 111, 154-161, https://doi.org/10.1016/j.still.2010.09.007

Kravchenko A.N., Wang A.N.W., Smucker A.J.M., and Rivers M.L., 2011. Long-term differences in tillage and land use affect intra-aggregate pore heterogeneity. Soil Sci. Soc. Am. J., 75, 1658-1666, https://doi.org/10.2136/sssaj2011.0096

Lamandé M., Wildenschild D., Berisso F.E., Garbout A., Marsh M., Moldrup P., Keller T., Hansen S.B., De Jonge L.W., and Schjønning P., 2013. X-ray CT and laboratory measurements on glacial till subsoil cores: Assessment of inherent and compaction-affected soil structure characteristics. Soil Sci., 178(7), 359-398, https://doi.org/10.1097/SS.0b013e3182a79e1a

Larsbo M., Koestel J., and Jarvis N., 2014. Relations between macropore network characteristics and the degree of preferential solute transport. Hydrol. Earth Syst. Sci., 18, 5255-5269, https://doi.org/10.5194/hess-18-5255-2014

Lauber C.L., Strickland M.S., Bradford M.A., and Fierer N., 2008. The influence of soil properties on the structure of bacterial and fungal communities across land-use types. Soil Biol. Biochem., 40, 2407-2415, https://doi.org/10.1016/j.soilbio.2008.05.021.

Leuther F., Schlüter S., Wallach R., and Vogel H.J., 2019. Structure and hydraulic properties in soils under long-term irrigation with treated wastewater. Geoderma, 333, 90-98, https://doi.org/10.1016/j.geoderma.2018.07.015.

Lin H., Brooks E., McDaniel P., and Boll J., 2008. Hydropedology and Surface/Subsurface Runoff Processes. Encycl. Hydrol. Sci., https://doi.org/10.1002/0470848944.hsa306

Liu Z., Ma D., Hu W., and Li X., 2018. Land use dependent variation of soil water infiltration characteristics and their scale-specific controls. Soil Tillage Res., 178, 139-149, https://doi.org/10.1016/j.still.2018.01.001

Luo L., Lin H., and Li S., 2010a. Quantification of 3-D soil macropore networks in different soil types and land uses using computed tomography. J. Hydrol., 393, 53-64, https://doi.org/10.1016/j.jhydrol.2010.03.031

Luo L., Lin H., and Schmidt J., 2010b. Quantitative relationships between soil macropore characteristics and preferential flow and transport. Soil Sci. Soc. Am. J., 74, 1929-1937, https://doi.org/10.2136/sssaj2010.0062

Murty D., Kirschbaum M.U.F., McMurtrie R.E., and McGilvray H., 2002. Does conversion of forest to agricultural land change soil carbon and nitrogen? A review of the literature. Glob. Chang. Biol., 8, 105-123, https://doi.org/10.1046/j.1354-1013.2001.00459.x

de Oliveira J.A.T., Cássaro F.A.M., and Pires L.F., 2021. Estimating soil porosity and pore size distribution changes due to wetting-drying cycles by morphometric image analysis. Soil Tillage Res., 205, 104814, https://doi.org/10.1016/j.still.2020.104814

Pagliai M., Vignozzi N., and Pellegrini S., 2004. Soil structure and the effect of management practices. Soil Tillage Res., 79(2), 131-143, http://doi.org/10.1016/j.still.2004.07.002

Price K., Jackson C.R., and Parker A.J., 2010. Variation of surficial soil hydraulic properties across land uses in the southern Blue Ridge Mountains, North Carolina, USA. J. Hydrol., 383, 256-268, https://doi.org/10.1016/j.jhydrol.2009.12.041

Qiao J., Liu X., Zhu Y., Jia X., and Shao M., 2021. Three-dimensional quantification of soil pore structure in wind-deposited loess under different vegetation types using industrial X-ray computed tomography. Catena, 199, 105098, https://doi.org/10.1016/j.catena.2020.105098

Rabot E., Wiesmeier M., Schlüter S., and Vogel H.J., 2018. Soil structure as an indicator of soil functions: A review. Geoderma, 314, 122-137, https://doi.org/10.1016/j.geoderma.2017.11.009

Rezanezhad F., Quinton W.L., Price J.S., Elrick D., Elliot T.R., and Heck R.J., 2009. Examining the effect of pore size distribution and shape on flow through unsaturated peat using computed tomography. Hydrol. Earth Syst. Sci., 13, 1993-2002, https://doi.org/10.5194/hess-13-1993-2009

Schlüter S., Eickhorst T., and Mueller C.W., 2019. Correlative Imaging Reveals Holistic View of Soil Microenvironments. Environ. Sci. Technol., 53, 829-837, https://doi.org/10.1021/acs.est.8b05245

Schlüter S., Großmann C., Diel J., Wu G.M., Tischer S., Deubel A., and Rücknagel J., 2018. Long-term effects of conventional and reduced tillage on soil structure, soil ecological and soil hydraulic properties. Geoderma, 332, 10-19, https://doi.org/10.1016/j.geoderma.2018.07.001

Schlüter S., Sheppard A., Brown K., and Wildenschild D., 2014. Image processing of multiphase images obtained via X-ray microtomography: A review. Water Resour. Res., 50(4), 3615-3639, https://doi.org/10.1002/2014WR015256

Shabtai I.A., Shenker M., Edeto W.L., Warburg A., and Ben-Hur M., 2014. Effects of land use on structure and hydraulic properties of Vertisols containing a sodic horizon in northern Ethiopia. Soil Tillage Res., 136, 19-27, https://doi.org/10.1016/j.still.2013.09.007

Tabor Z., 2011. A novel method of estimating structure model index from gray-level images. Med. Eng. Phys., 33, 218-225, https://doi.org/10.1016/j.medengphy.2010.10.005

Udawatta R.P., and Anderson S.H., 2008. CT-measured pore characteristics of surface and subsurface soils influenced by agroforestry and grass buffers. Geoderma, 145, 381-389, https://doi.org/10.1016/j.geoderma.2008.04.004

Udawatta R.P., Anderson S.H., Gantzer C.J., and Garrett H.E., 2008. Influence of prairie restoration on CT-measured soil pore characteristics. J. Environ. Qual., 37, 219-228, https://doi.org/10.2134/jeq2007.0227

Vogel H.J., 2000. A numerical experiment on pore size, pore connectivity, water retention, permeability, and solute transport using network models. Eur. J. Soil Sci., 51, 99-105, https://doi.org/10.1046/j.1365-2389.2000.00275.x

Walkley A. and Black I.A., 1934. An examination of the Degtjareff method for determining soil organic matter, and a proposed modification of the chromic acid titration method. Soil Sci., 37(1), 29-38, https://doi.org/10.1097/00010694-193401000-00003

Wang M., Xu S., Kong C., Zhao Y., Shi X., and Guo N., 2019. Assessing the effects of land use change from rice to vegetable on soil structural quality using X-ray CT. Soil Tillage Res., 195, 104343, https://doi.org/10.1016/j.still.2019.104343

Woolhiser D.A., Fedors R.W., Smith R.E., and Stothoff S.A., 2006. Estimating Infiltration in the Upper Split Wash Watershed, Yucca Mountain, Nevada. J. Hydrol. Eng., 11, 123-133, https://doi.org/10.1061/(asce)1084-0699(2006)11:2(123)

Zeng C., Zhang F., Wang Q., Chen Y., and Joswiak D.R., 2013. Impact of alpine meadow degradation on soil hydraulic properties over the Qinghai-Tibetan Plateau. J. Hydrol., 478, 148-156, https://doi.org/10.1016/j.jhydrol.2012.11.058

Zhang Z., Lin L., Wang Y., and Peng X., 2016. Temporal change in soil macropores measured using tension infiltrometer under different land uses and slope positions in subtropical China. J. Soils Sediments, 16, 854-863, https://doi.org/10.1007/s11368-015-1295-z

Zhang Z., Liu K., Zhou H., Lin H., Li D., and Peng X., 2018. Three dimensional characteristics of biopores and non-biopores in the subsoil respond differently to land use and fertilization. Plant Soil, 428, 453-467, https://doi.org/10.1007/s11104-018-3689-3

Zhang Z., Liu K., Zhou H., Lin H., Li D., and Peng X., 2019. Linking saturated hydraulic conductivity and air permeability to the characteristics of biopores derived from X-ray computed tomography. J. Hydrol., 571, 1-10, https://doi.org/10.1016/j.jhydrol.2019.01.041

Zhao D., Xu M., Liu G., Ma L., Zhang S., Xiao T., and Peng G., 2017. Effect of vegetation type on microstructure of soil aggregates on the Loess Plateau, China. Agric. Ecosyst. Environ., 242, 1-8, https://doi.org/10.1016/j.agee.2017.03.014

Zhou X., Lin H.S., and White E.A., 2008. Surface soil hydraulic properties in four soil series under different land uses and their temporal changes. Catena, 73, 180-188, https://doi.org/10.1016/j.catena.2007.09.009

Zhu S., Zhen Q., and Zhang X., 2020. Multifractal characteristics of the pore structures of physically amended sandy soil and the relationship between soil properties and multifractal parameters. Arch. Agron. Soil Sci., 66, 1188-1202, https://doi.org/10.1080/03650340.2019.1660960